Infrared Excitation of Visible Luminescence in $Y_{1-x}Er_xF_3$ via Resonant Energy Transfer

J. P. VAN DER ZIEL, F. W. OSTERMAYER, JR., AND L. G. VAN UITERT
Bell Telephone Laboratories, Murray Hill, New Jersey 07974

(Received 14 May 1970)

The temperature and concentration dependences of the visible emission of Er^{3+} in YF_3 under infrared excitation of the $^4I_{11/2}$ levels have been measured. The infrared radiation is absorbed by ions initially in the ground state and two excitations subsequently combine, yielding an ion in a higher-energy state. The temperature dependence of the $^4S_{3/2}\rightarrow{}^4I_{15/2}$ emission has a broad maximum at 90°K. The reduction in the emission for $T<90$°K results from the depopulation of the higher-energy crystal-field-split levels of the $^4I_{11/2}$ manifold which have a resonant match with the $^4F_{7/2}$ levels. For $T>90$°K the emission is increasingly quenched by ion-pair relaxation from $^4S_{3/2}$ via $^2H_{11/2}$. For the concentration range $0.01<x<0.1$, the $^4S_{3/2}$ emission is proportional to $x^{2.9}$ at 77°K and to $x^{1.3}$ at 295°K.

I. INTRODUCTION

The visible emission observed from Er^{3+} using infrared excitation results from absorption by two separate ions in the ground state, and subsequent coalescence of the two excitations by transfer to a single ion.[1–4] For the red and green emission we show that this mechanism is several orders of magnitude more effective than the usual quantum-counter scheme, which involves the sequential absorption of two infrared photons by a single ion. In general, however, both mechanisms are operative.

Auzel found that the addition of Yb^{3+} greatly enhances the conversion efficiency and attributed the enhancement to the transfer process.[5] In the Yb^{3+}-Er^{3+} system the infrared radiation is predominantly absorbed by the $^2F_{7/2}$ to $^2F_{5/2}$ transition of the Yb^{3+} sensitizer, and the higher-lying Er^{3+} levels from which the fluorescence originates are populated by the sequential transfer of excitation from two Yb^{3+} ions to one Er^{3+} ion. Up-conversion of infrared radiation has also been investigated in Yb^{3+}-Ho^{3+} and Yb^{3+}-Tm^{3+} compositions. As many as four consecutive transfers have been observed.[6–12]

In this paper we present the results of several infrared to visible conversion experiments of Er^{3+} in YF_3. Our primary aim is to obtain a better understanding of the characteristics of the two-photon up-conversion processes resulting from the infrared excitation of the Er^{3+} $^4I_{15/2}\rightarrow{}^4I_{11/2}$ transition. The results of this study are also pertinent to other up-conversion processes; in particular, since the same Er^{3+} energy levels are involved, they apply directly to the Yb→Er transfer in (Y YbEr)F_3.

II. EXPERIMENTAL

A. Sample Preparation

The phosphors were prepared[12] by converting 99.9999% purity Y_2O_3 and 99.999% purity Er_2O_3 to fluorides by dissolving the oxides in HNO_3, precipitating with an excess of HF, dehydrating by evaporation at room temperature, mixing the resulting powder with BeF_2 and NH_4F in a platinum crucible, covering the crucible and placing it in a muffle furnace preheated to 1100°C and allowing the furnace to cool. The BeF_2 is quite liquid above 800°C and encapsulates, dissolves, and crystallizes the phosphor, as well as scavenging any trace of oxide. The evaporation of the NH_4F flushes the air from the crucible. The crucible contents consists of lumps of small rare-earth fluoride crystallites and glassy flux. The fine phosphor powders used in our experiments were obtained by grinding the lumps. Since the flux makes up a small fraction of the total mass, and its presence does not affect the relative intensity measurements described here, no attempt was made to separate it from the crystallites. The Er^{3+} and Y^{3+} concentrations were determined by spectrochemical analysis.

Yttrium fluoride is orthorhombic and belongs to the D_{2h}^{16} space group.[13] There are four formula units in the unit cell. The trivalent rare-earth ions substitute on the yttrium sites without charge compensation. The heavier rare-earth ions are soluble over the complete concentration range with no resulting change in crystal structure.

B. Spectroscopy

The Er^{3+} energy levels are shown in Fig. 1. The positions of several of the Stark components have been determined from low-temperature fluorescence and excitation spectra by the usual spectroscopic techniques, and are given in Table I. Typical spectra are shown in Figs. 2 and 3. Figure 2(a) shows the 295°K $^4S_{3/2}\rightarrow{}^4I_{15/2}$ green emission at 0.54 μ as the excitation is swept through the $^4I_{15/2}\rightarrow{}^4I_{11/2}$ infrared transition. The emission is very similar to the reflectance spectrum of the latter transition, which is shown in Fig. 2(b). Figure 2(c) shows the relative $^4I_{11/2}\rightarrow{}^4I_{15/2}$ emission obtained by pumping the $^4F_{7/2}$ states which are at twice the $^4I_{11/2}$ states.

The spectra were obtained using a 1-m Czerny-Turner spectrometer equipped with a 200-W tungsten source. The emission from $^4S_{3/2}$ and $^4I_{11/2}$ was detected with *S*-20 and *S*-1 response photomultipliers, respec-

tively, and a cooled PbS cell was used to detect the infrared reflectivity.

The spectra at 77°K are shown in Fig. 3. On cooling the absorption shifts to higher energy, due to the thermal depopulation of the upper $^4I_{15/2}$ levels, and the lines become appreciably narrower. The relative intensities and the energies of the transitions are found to be relatively independent of concentration.

Theory predicts the $^4S_{3/2}$ emission to be proportional to the square of the pump power absorbed. A plot of the $^4S_{3/2}$ emission as a function of the infrared absorption A, determined from $A=1-R$, where R is the reflectance, was obtained from sharp-line spectra similar to Figs. 3(a) and 3(b) and is shown by the open points in Fig. 4. The emission has the expected quadratic dependence on absorption for $A<0.45$, but deviates significantly from this dependence for the stronger transitions. Similar curves were obtained when the ir intensity was attenuated up to a factor 4 with neutral density filters. Hence for a given concentration, the deviation from square-law behavior is independent of the density of ions in the $^4I_{11/2}$ state.

The deviation from a quadratic dependence can be understood by idealizing the phosphor-powder plaque to a thin uniform crystal plate of thickness d and attenuation α per cm. The fraction of light absorbed in passing through the plate is

$$A=1-I(d)/I(0)=1-e^{-\alpha d}, \qquad (1)$$

where $I(0)$ and $I(d)$ are the incident and transmitted intensities. Assuming negligible reabsorption and scattering, the usual fluorescence is given by

$$E_1 \propto \int_0^d \frac{dI(y)}{dy}\,dy \propto I(0)A, \qquad (2)$$

which yields the linear dependence observed in Fig. 4. For ir excitation, the fluorescence generated a distance y from the front surface is proportional to $[dI(y)/dy]^2$ and the total emission is

$$E_2 \propto \int_0^d \left(\frac{dI(y)}{dy}\right)^2 dy \propto -I(0)^2A(2-A)d^{-1}\ln(1-A). \qquad (3)$$

The fluorescence E_2 is proportional to $I(0)^2d^{-1}A^2$ for $A<0.7$ and increases more rapidly for $A>0.7$. The observed deviation occurs at lower values of absorption for two reasons. The reflectivity and excitation measurements were made using the same spectrometer slit width, which, however, was not sufficiently small to fully resolve the sharpest lines. Thus the true values of A, especially for stronger lines, are larger than the measured quantities. This was confirmed by repeating the measurements using progressively larger slit widths which further decreased the measured A values, and

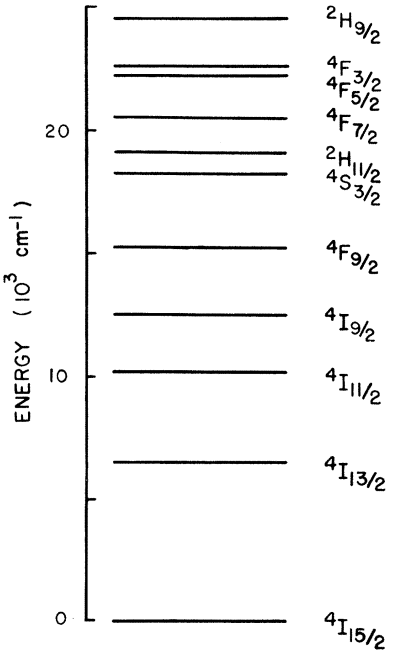

FIG. 1. Energy levels of Er^{3+}.

TABLE I. Energy levels of Er^{3+} in YF_3 at 77°K.

SLJ		Energy (cm^{-1})	SLJ		Energy (cm^{-1})
$^4I_{15/2}$	$Z1$	0	$^4F_{9/2}$	$D1$	15 336.5
	$Z2$	90.0		$D2$	15 386.4
	$Z3$	130.5		$D3$	15 394.2
	$Z4$	175.8		$D4$	15 471.6
	$Z5$	194.2		$D5$	15 486.6
	$Z6$	249.0	$^4S_{3/2}$	$E1$	18 490.8
	$Z7$	347.6		$E2$	18 572.2
	$Z8$	429.3			
			$^2H_{11/2}$	$F1$	19 228.8
$^4I_{11/2}$	$A1$	10 254.2			
				$F2$	19 265.5
	$A2$	10 277.4			
				$F3$	19 281.5
	$A3$	10 314.3			
				$F4$	19 309.2
	$A4$	10 333.1			
				$F5$	19 323.4
	$A5$	10 343.1			
				$F6$	19 356.6
	$A6$	10 366.1			
			$^4F_{7/2}$	$G1$	20 586.5
				$G2$	20 642.6
				$G3$	20 676.8
				$G4$	20 762.2

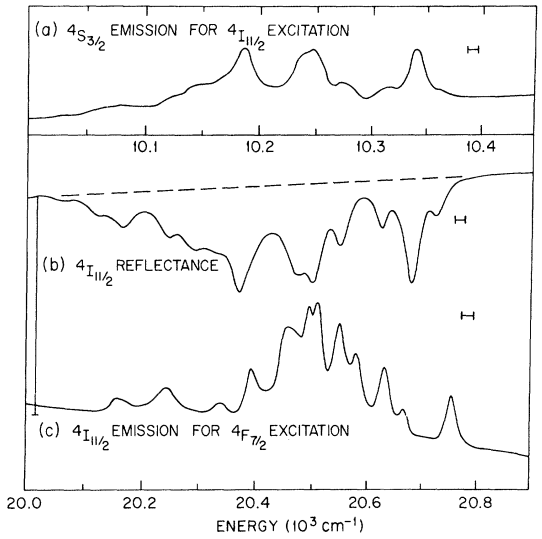

FIG. 2. Spectra of $Y_{0.9}Er_{0.1}F_3$ at 295°K. (a) Infrared excitation spectrum of $^4S_{3/2}$ fluorescence. (b) Reflectance spectrum corresponding to the $^4I_{15/2}\rightarrow{}^4I_{11/2}$ transition. (c) The $^4F_{7/2}$ excitation spectrum of $^4I_{11/2}$ fluorescence.

caused the deviation from a quadratic dependence to shift to smaller absorption. Secondly, the above analysis applies to a single crystal plate, whereas for the phosphor plaque the average effective thickness, which can be obtained from a knowledge of A and α using Eq. 1, is determined by the scattering of the light within the powder and the absorption coefficient α. For larger values of α such that $\alpha^{-1}\sim d$, the effective thickness is

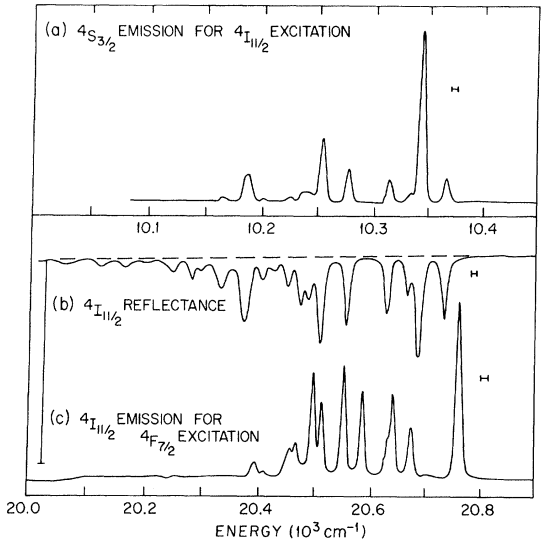

FIG. 3. Spectra of $Y_{0.9}Er_{0.1}F_3$ at 77°K. (a) Infrared excitation spectrum of $^4S_{3/2}$ fluorescence. (b) Reflectance spectrum corresponding to the $^4I_{15/2}\rightarrow{}^4I_{11/2}$ transition. (c) The $^4F_{7/2}$ excitation spectrum of $^4I_{11/2}$ fluorescence.

smaller than the value in the absence of absorption. This does not affect E_1 explicitly; however, E_2 is enhanced by the smaller value of d in the denominator of Eq. 3. In $(LaYbEr)F_3$ Hewes and Sarver have also observed a nonquadratic dependence of the Er^{3+} emission on the Yb^{3+} infrared absorption spectrum.[6] The Yb^{3+} absorption consists of several broad bands, and in the region of strong absorption the best fit to the excitation spectrum was given by the cube of the absorption.[14]

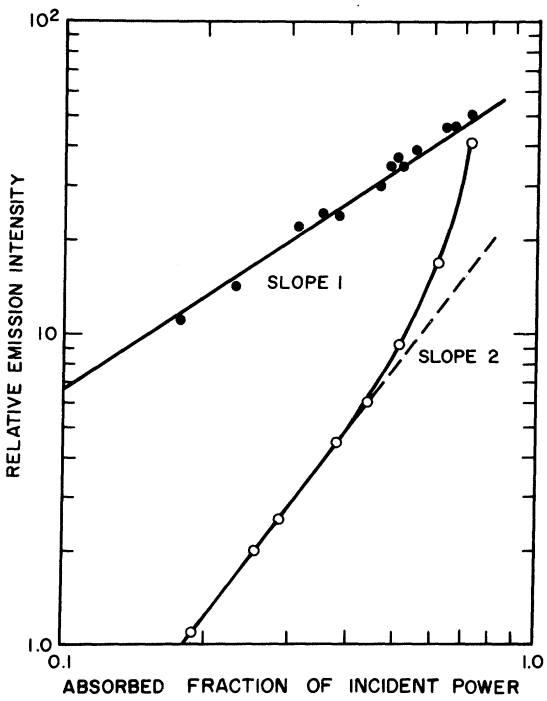

FIG. 4. Dependence of the emission intensity as a function of absorbed power at 77°K. The open points give the $^4S_{3/2}$ emission for the absorption of the $^4I_{13/2}\rightarrow{}^4I_{11/2}$ transitions of $Y_{0.9}Er_{0.1}F_3$ obtained from Figs. 3(a) and 3(b). The solid points give the $^4F_{9/2}$ emission for several of the $^4I_{15/2}\rightarrow{}^4F_{7/2}$ transitions in $Y_{0.7}Er_{0.3}F_3$.

C. Temperature Dependence

The dependences of the $^4S_{3/2}$ emission intensity on temperature for the 2.5% and 10% phosphors are shown in Figs. 5 and 6 for the case when the excitation is, respectively, into the $^4F_{7/2}$ and $^4I_{11/2}$ levels. For these measurements, the excitation source consisted of a Bausch and Lomb spectrometer with an infrared grating and standard tungsten light source. This instrument passed a 120 Å band centered at 4800 Å and a 250 Å band centered at 9700 Å. The higher orders were removed using glass filters. The fluorescence was isolated with a second Bausch and Lomb spectrometer and glass filters. The temperature, measured with a copper constantan thermocouple, and the emission were continuously monitored as the phosphor slowly warmed up from 20°K. Temperatures above 295°K were ob-

tained with a small heater placed near the phosphor. As shown in Fig. 5, with increasing temperature the emission initially increases, reaches a maximum, and then decreases. The dependence at low temperatures is similar for both concentrations and results from the thermal population of the higher-energy $^4I_{15/2}$ crystal-field levels which (Figs. 2 and 3) have higher absorption strengths to $^4F_{7/2}$ than the lowest-energy level. Nonradiative decay is important above 100°K. This consists primarily of the thermal excitation to $^2H_{11/2}$ and the subsequent decay predominantly to lower levels via the ion-pair processes

$$(^2H_{11/2}, {}^4I_{15/2}) \rightarrow (^4I_{9/2}, {}^4I_{13/2})$$

and

$$(^2H_{11/2}, {}^4I_{15/2}) \rightarrow (^4I_{13/2}, {}^4I_{9/2}).$$

The thermal population of $^2H_{11/2}$ and hence the decay is enhanced by the factor 3 greater degeneracy of this level. Although the dominant decay is from $^2H_{11/2}$, at higher temperatures there are additional possible contributions from stimulated multiphonon decay directly from $^4S_{3/2}$ and following thermal excitation to $^4F_{7/2}$, ion-pair relaxation

$$(^4F_{7/2}, {}^4I_{15/2}) \rightarrow (^4I_{11/2}, {}^4I_{11/2}).$$

With increasing concentration, the peak of the emission shifts to lower temperature, and the effects of nonradiative decay become more pronounced at the temperatures just above the maximum intensity. For the 2.5% phosphor, thermally excited ion-pair decay is predominant above 250°K and the emission has the same temperature dependence as the 10% concentration. At the lowest temperatures, the thermal excitation from $^4S_{3/2}$ is greatly reduced. However, the intensity increases only by a factor 2, rather than the fourfold increase predicted from the ratio of the concentrations; hence there is a concentration-dependent decay which, in bypassing the $^4S_{3/2}$ level, competes with the nonradiative $^4F_{7/2} \rightarrow {}^4S_{3/2}$ transition.

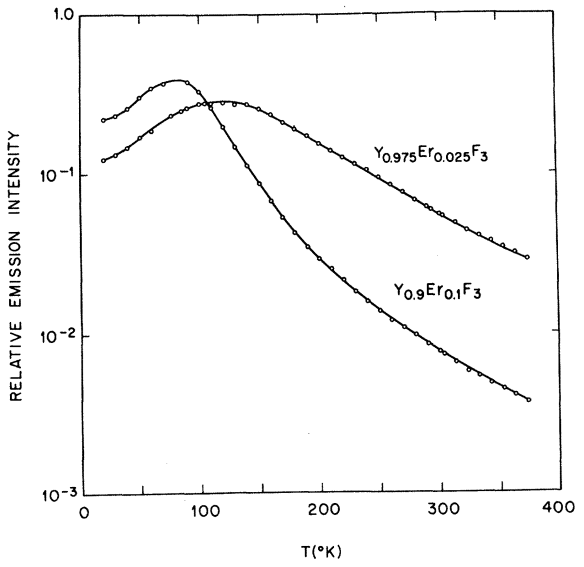

FIG. 5. Temperature dependence of the $^4S_{3/2}$ intensity for $^4F_{7/2}$ excitation.

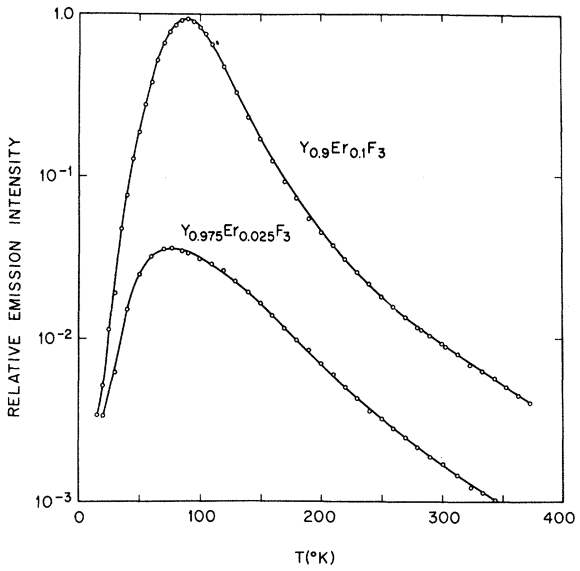

FIG. 6. Temperature dependence of the $^4S_{3/2}$ intensity for $^4I_{11/2}$ excitation.

Significant differences are observed for the temperature dependence of the $^4I_{11/2}$ excited emission shown in Fig. 6. First, the decrease of the emission at low temperatures is striking confirmation of the resonant nature of the energy transfer mechanism. From Table I there are 13 cases where the energy difference between $^4I_{11/2}$-$^4I_{15/2}$ and $^4F_{7/2}$-$^4I_{11/2}$ is less than 4 cm^{-1} and eight cases where the mismatch is between 4 and 10 cm^{-1}. Since the minimum linewidth is about 4 cm^{-1} at 77°K, the overlap of the first group is almost perfect, and appreciable for the second.

Each of the $^4I_{11/2}$ levels is involved in at least one resonance. For example, when one of the ions is in $A1$ the only match occurs with the second ion in $A4$. The energy difference of this pair with a single ion in the $G1$ level of $^4F_{7/2}$ is 0.8 cm^{-1}. When both ions are in the $A1$ level the mismatch is 78.1 cm^{-1}. The decrease in the emission at low temperatures is thus explained by the reduction in resonant transfer which occurs because of the thermal depopulation of the higher-energy $^4I_{11/2}$ levels. The infrared source for these measurements is sufficiently broad to include both the $^4I_{15/2} \rightarrow {}^4I_{11/2}$ and the $^4I_{11/2} \rightarrow {}^4F_{7/2}$ transitions and the process of consecutive absorption by one ion would not have this temperature dependence.

Secondly, between 100 and 295°K the quenching of the emission is more effective than occurs for excitation into $^4F_{7/2}$. This is the result of the difference in the method of excitation. The enhanced quenching with infrared excitation occurs because the transfer of the

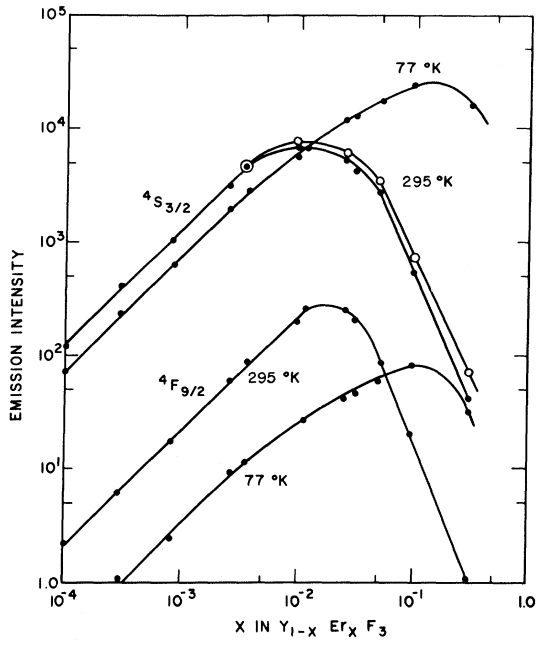

FIG. 7. Concentration dependence of $^4S_{3/2}$ and $^4F_{9/2}$ emission for $^4F_{7/2}$ excitation.

excitation to a single ion is most likely for a relatively tightly coupled pair, and it is just such pairs that have a high probability to relax back to the ^4I_J levels again. For $^4F_{7/2}$ excitation, the emission is mainly from relatively isolated ions for which the probability of ion-pair relaxation is reduced. For the two modes of excitation, the difference in the ion-pair relaxation is greatest for the 2.5% phosphor, since this composition contains a higher concentration of relatively isolated ions.

D. Concentration Dependence

The emission from the $^4S_{3/2}$ and $^4F_{9/2}$ levels was measured over the concentration range from 10^{-4} to 0.3. Figure 7 shows the dependence when the $^4F_{7/2}$ manifold is excited. The intensity curves are typical of the concentration dependence of Er^{3+} found in other hosts.[15] The maxima in the emission occurs for 1% at 300°K and for 10% at 77°K. The shift to higher concentration is due to the decrease in nonradiative decay resulting from the thermal depopulation of $^2H_{11/2}$. For concentrations below 1% the intensity decreases as the temperature is lowered. As seen from Figs. 2(c) and 3(c), the decrease is primarily due to the thermal depopulation of the excited $^4I_{15/2}$ crystal-field levels and the resulting decrease in the $^4I_{15/2}\rightarrow{}^4F_{7/2}$ absorption.

The concentration dependence of the intensity from the $^4S_{3/2}\rightarrow{}^4I_{13/2}$ transition when the excitation is directly into $^4S_{3/2}$ is shown by the open points in Fig. 7. The intensities of this curve have been normalized to bring the point for the 0.35% concentration into coincidence with the $^4F_{7/2}$ curve. The $^4S_{3/2}$ emission data for excitation into $^4F_{7/2}$ exhibits a slightly stronger concentration-dependent quenching. The difference between the two curves is a measure of the ion-pair decay which results during the cascade from $^4F_{7/2}\rightarrow{}^4S_{3/2}$ compared to the nonradiative single ion decay between these two levels. Except for the highest concentration this gives a small contribution to the quenching. Thus the nonradiative decay occurs *after* the ion has relaxed to $^4S_{3/2}$. The similarity of the $^4F_{9/2}$ and $^4S_{3/2}$ curves and their temperature dependences show that the $^4F_{9/2}$ level is populated by thermally excited multiphonon decay from $^4S_{3/2}$.

The concentration dependence of the emission for excitation into $^4I_{11/2}$ is shown in Fig. 8. The $^4S_{3/2}$ emission is separable into two concentration ranges. Up to 0.3% the intensity varies approximately linearly with concentration and $^4S_{3/2}$ is populated by the sequential absorption process. Above 0.3% the intensity increases superlinearly, and the resonant transfer mechanism is dominant.

On lowering the temperature, the reduction in ion-pair decay is relatively more important for the higher concentrations (Fig. 7). Consequently the concentration dependence of the emission due to up-transfer is a

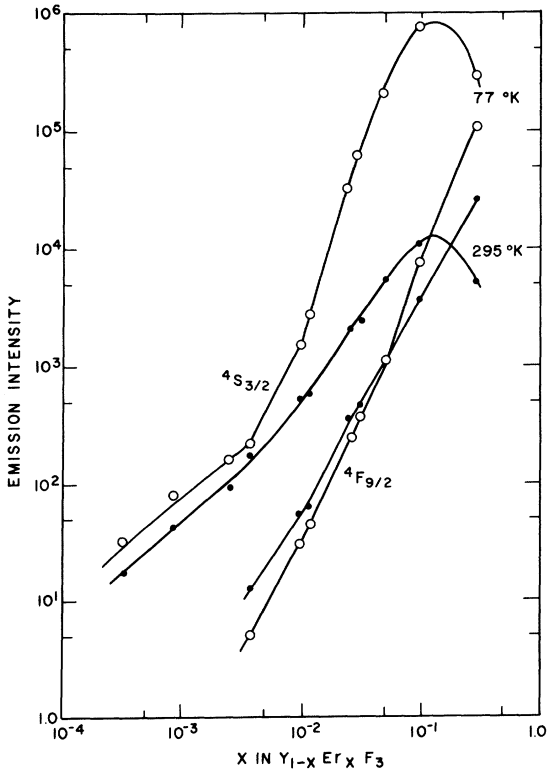

FIG. 8. Concentration dependence of the $^4S_{3/2}$ and $^4F_{9/2}$ emission for $^4I_{11/2}$ excitation.

function of temperature. For example, in Fig. 8 the 77°K emission has a dependence which is approximately cubic for the Er^{3+} range between 1% and 10%. Previously Feofilov and Ovsyankin found that the infrared excited green emission of Er^{3+} in single-crystal BaF_2 varies as the square of the concentration at 300°K for the same concentration range.[1] This was taken by them to be the characteristic dependence of the up-transfer. From Fig. 8 the dependence at 295°K is less than quadratic. It is evident from this discussion that the dependence observed at 295°K is the net result of the up-transfer process starting at about 0.3% and the partial cancellation by the ion-pair relaxation beginning at about 1% and is not characteristic of the up-transfer process alone.

Under infrared excitation, the $^4F_{9/2}$ level may be populated via two routes. The first consists of direct nonradiative decay from $^4S_{3/2}$, as was found when the $^4F_{7/2}$ level was excited. For the second route, the $^4I_{13/2}$ level at 1.53 μ is first populated either by direct decay from $^4I_{11/2}$ or by ion-pair decay from $^2H_{11/2}$ and this excitation combines with a $^4I_{11/2}$ excitation to yield a single ion in $^4F_{9/2}$ and liberating about 1400 cm^{-1} to the lattice. As is seen from Figs. 7 and 8, the relative intensities from $^4F_{9/2}$ and $^4S_{3/2}$ when the $^4F_{7/2}$ or $^4I_{11/2}$ levels are excited shows the $^4F_{9/2}$ emission is appreciably stronger for $^4I_{11/2}$ excitation. Thus the emission comes mainly from the second route. Furthermore, the temperature dependence of the $^4F_{9/2}$ emission indicates that the $^4I_{13/2}$ level is populated largely by direct decay from $^4I_{11/2}$.

A final point concerns the smaller green emission obtained from the 30% as compared to the 10% phosphor. The decrease is sufficient to make the 300°K emission from the concentrated compound appear visually red, whereas the remaining compounds at 300°K and all the compounds at 77°K produce a green visual sensation. The decrease in the green intensity is in part due to the reduction in the $^4I_{11/2}$ equilibrium population which follows from the shorter lifetime of the 30% concentration. The more rapid decay from $^4I_{11/2}$ enhances the $^4I_{13/2}$ population, and this compensates for the decrease in the $^4I_{11/2}$ population, so that the probability for upward transfer to $^4F_{9/2}$ is essentially unchanged.

The dependence of the emission on the pump power was obtained for the 1, 10, and 30% concentrations. Over a pump intensity range of one decade, the $^4S_{3/2}$ and $^4F_{9/2}$ emission varied as the square of the pump power.

E. Lifetimes

The concentration dependences of the lifetimes are shown in Fig. 9. The lifetimes were obtained from the e^{-1} decay of the emission following pulsed excitation into the level to be measured. The $^4S_{3/2}$ decay was also measured for excitation into $^2H_{11/2}$ and $^4F_{7/2}$ and was

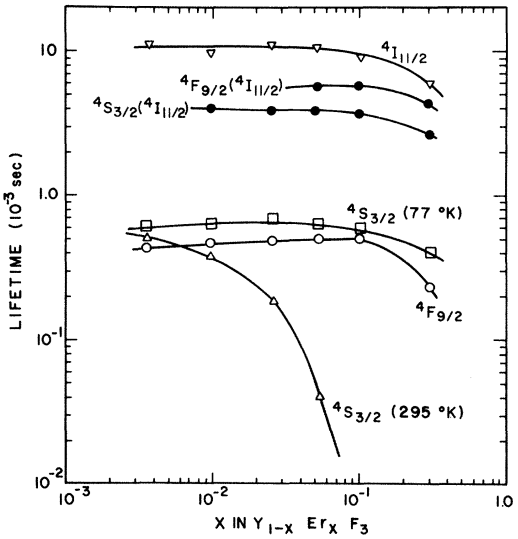

FIG. 9. Concentration dependence of the fluorescence lifetimes. The lifetimes of the $^4S_{3/2}$ and $^4F_{9/2}$ fluorescence for $^4I_{11/2}$ excitation are denoted by the solid points.

the same as for direct excitation into $^4S_{3/2}$. Thus the decay from these levels to $^4S_{3/2}$ is shorter than the 5×10^{-6} sec duration of the flash. The concentration dependences of the $^4S_{3/2}$ lifetimes at 300 and 77°K agrees with the degree of quenching of the emission from this level. Up to a 10% doping, the lifetimes of $^4S_{3/2}$ at 77°K and of $^4I_{11/2}$ and $^4F_{9/2}$ are relatively independent of concentration. These values are in good agreement with the lifetimes of Er^{3+} in LaF_3.[16]

The lifetimes of the $^4S_{3/2}$ and $^4F_{9/2}$ emission for excitation into $^4I_{11/2}$ are shown in Fig. 9 by the solid points. The source for these measurements was a silicon-doped GaAs diode (Texas Instruments type OSX 1208) emitting in a 450 Å band centered at 9300 Å. The phosphors were attached directly to the dome of the diode with collodion. The lifetimes were obtained from the decay of the emission following a 10^{-2} sec current pulse. This is sufficiently long for the transient behavior, observed with very short pulses, to have been damped out, and the populations to have reached the steady-state values corresponding to a steady-state incident infrared flux. The decay of the emission from $^4I_{11/2}$ is exponential. Using the fact that $\tau(^4S_{3/2})\ll\tau(^4I_{11/2})$, the solution of the time-dependent rate equations for the lifetime of the $^4S_{3/2}$ emission under $^4I_{11/2}$ excitation yields

$$\tau'(^4S_{3/2})=\tfrac{1}{2}\tau(^4I_{11/2}). \tag{4}$$

The situation for the $^4F_{9/2}$ emission is somewhat more complicated because the $^4I_{13/2}$ level is involved. This level is populated by decay from $^4I_{11/2}$. However, Weber has shown that for LaF_3:Er^{3+} the $^4I_{11/2}\rightarrow{}^4I_{13/2}$

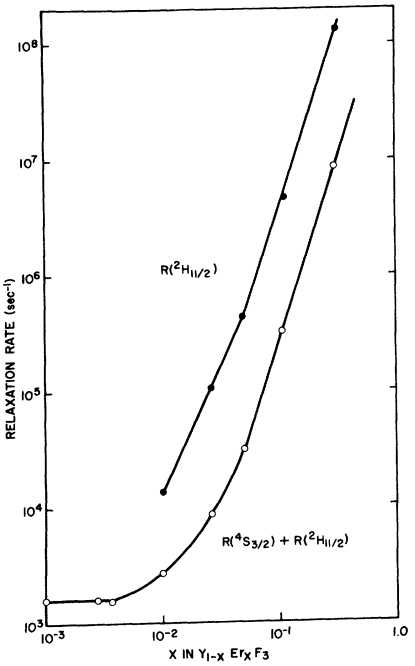

FIG. 10. Concentration dependence of the 295°K decay rates. Open points: combined decay from $^4S_{3/2}$ and $^2H_{11/2}$; closed points: ion-pair decay from $^2H_{11/2}$.

transition accounts for less than 20% of the total decay from $^4I_{11/2}$, the remaining going to the $^4I_{15/2}$ level.[16] Since the properties of Er^{3+} in the two hosts are very similar, it is not unreasonable to assume that the above branching ratio applies also to the YF_3 host. Hence, during the initial part of the decay, we can to a first approximation neglect the continuing transfer from $^4I_{11/2}$ to $^4I_{13/2}$. Under these conditions we obtain, noting that $\tau(^4F_{9/2}) \ll \tau(^4I_{11/2}), \tau(^4I_{13/2})$,

$$\tau'(^4F_{9/2})^{-1} = \tau(^4I_{11/2})^{-1} + \tau(^4I_{13/2})^{-1}. \quad (5)$$

The diode operates at a somewhat elevated temperature, and the associated heating of the phosphor results in a reduction of the $^4I_{11/2}$ lifetime. The measured $^4S_{3/2}$ lifetime is somewhat smaller than half of the $^4I_{11/2}$ lifetime obtained from flash excitation. The $^4I_{13/2}$ lifetime of 0.013 sec is less temperature dependent, and the agreement with Eq. (5) is excellent.

III. DISCUSSION

A. Concentration Dependence of Ion-Pair Relaxation

The probability for energy transfer from ion i to ion j, which results in the up-conversion from $^4I_{11/2}$ to $^4F_{7/2}$ and ion-pair decay from $^2H_{11/2}$, is given by[17]

$$P_{ij} = \hbar^{-2} |H_{ij}|^2 \int g_i(\nu) g_j(\nu) d\nu. \quad (6)$$

Here H_{ij} is the matrix element of the Hamiltonian between the initial and final states of the interacting pair and the integral is the overlap of the normalized line shape function $g(\nu)$. The coupling results from either electrostatic multipole interactions or exchange. For cases where there is no direct overlap, energy transfer can occur by phonon assistance.[18] We first consider the ion-pair decay process. In much of the previous work the radial dependence of the transfer interaction has been determined from the concentration dependence of the emission and lifetimes.[19] For quenching via multipolar interactions the concentration dependence of the emission per ion is given asymptotically by

$$I/I_0 = [1+\beta(x/x_0)^{\theta/3}]^{-1}, \quad (7)$$

where β is a constant which depends on the type of interaction and $\theta = 6$, 8, and 10 for dipole-dipole, dipole-quadrupole, and quadrupole-quadrupole interactions, respectively. Recently Birgeneau has questioned the identification of the transfer mechanism from the concentration dependence.[20] He was able to show that in ruby the transfer from single ions to pairs cannot be due to the quadrupole-quadrupole interaction, as is indicated by the concentration dependence, but is explainable on the basis of orbitally dependent exchange. Even taking into account the problems associated with identifying the transfer mechanism from the concentration dependence we still expect the transfer rate to depend critically on the selection rules and the magnitude of the interaction Hamiltonian, as well as the degree of overlap of the emission and absorption. However, for several resonant ion-pair transitions of Pr^{3+} and Nd^{3+}, Gandrud and Moos[21] found the quenching rates to a first approximation to have similar concentration dependences, varying as $x^{2.8}$. The relative independence on the above parameters may be associated with the resonant transfer being phonon-assisted.[22] The ions have natural linewidths which are appreciably smaller than the observed inhomogeneous widths; consequently, neighboring ions having transition energies that differ by more than the natural width have small overlap integrals and will not take part in the energy-transfer process. This mismatch may be mediated by the phonon interaction. Since the phonon density of states is very small at low energies, the most likely process involves the emission of a high-energy phonon at one ion site, and the absorption of a phonon by the second ion.

Still another interaction mechanism involves the excitation of a virtual exciton of the host lattice.[23] This transfer mechanism has a range of the order of four lattice spacings.[24] However, the importance of this interaction for rare-earth systems has not definitely been established.

The concentration dependence of the combined relaxation rate from the $^4S_{3/2}$ and $^2H_{11/2}$ manifolds at 295°K is obtained from the $^4S_{3/2}$ data of Figs. 7 and 9 using

$$R(x) = R(x')[I(x')/I(x)](x/x'), \quad (8)$$

and is shown by the open circles in Fig. 10. Here the

intensity $I(x')$ and the relaxation rate $R(x')$ are the low-concentration values where $R(x')$ is concentration independent.

Let $R(^4S_{3/2})$ and $R(^2H_{11/2})$ be the average decay rates from $^4S_{3/2}$ and $^2H_{11/2}$. Under $^4S_{3/2}$ excitation, the population of the $^4S_{3/2}$ level $N(^4S_{3/2})$ is obtained from

$$WN=N(^4S_{3/2})[R(^4S_{3/2})+3R(^2H_{11/2})\exp(-\Delta E/kT)]. \quad (9)$$

Here W is the excitation rate and ΔE is the average energy separation between the levels defined by

$$N(^2H_{11/2})/N(^4S_{3/2}) = \sum_i \exp[-E_i(^2H_{11/2})/kT]/\sum_j \exp[-E_j(^4S_{3/2})/kT] \equiv 3\exp(-\Delta E/kT), \quad (10)$$

where the i and j sums span the Stark levels of the $^2H_{11/2}$ and $^4S_{3/2}$, respectively. This result assumes that thermal equilibrium exists between the $^4S_{3/2}$ and $^2H_{11/2}$ populations. The solid points in Fig. 10 are the decay rates from $^2H_{11/2}$ which are obtained by subtracting the concentration-independent rates and using the 295°K value of 0.07 of the population ratio equation (10). The rate varies as $x^{2.9\pm0.25}$. The concentration dependence and also the magnitude of the ion-pair rate are comparable to the rates found by Gandrud and Moos.[21] In terms of Eq. (7), this is describable as a dipole-quadrupole dependence.

B. Concentration Dependence of Up-Conversion

For the up-conversion process we consider the rate equations for a system consisting of the four relevant levels. We denote the populations by N_i, where $i=1$–4 refer to the $^4I_{15/2}$, $^4I_{11/2}$, $^4S_{3/2}$, and $^4F_{7/2}$ levels, respectively. Define the induced transition probability W_{12} between levels 1 and 2, and the spontaneous decay between levels i and j by R_{ij}, where $R_i=\sum_j R_{ij}$ is the total spontaneous downward transition rate from i. We extend our model by including in R_i the transition rates to the Er^{3+} levels which are not explicitly included in the four-level model, and furthermore include the $^2H_{11/2}$ decay rate in R_3. Let $C_{22,41}N_2^2$ be the upward transition from 2 to 4 and $C_{41,22}N_4N_1$ the ion-pair decay from 4 to 2. The transfer coefficients contain additional implicit concentration dependences which depend on the transfer mechanism. Then, under the condition of relatively inefficient operation where most of the population of 2 decays to 1 such that $R_2N_2\gg C_{22,41}N_2^2$, the emission intensity from level 3 under infrared excitation is given by

$$I_{31}=[(R_{31}/R_3)(R_{43}/R_4)(1+C_{41,22}N_1/R_4)^{-1}] \times(W_{12}/R_2)^2C_{22,41}N_1^2, \quad (11)$$

where $R_{31}{}^r$ is the radiative decay rate from 3 to 1. The factors in the brackets are identical to $^4S_{3/2}$ emission under $^4F_{7/2}$ excitation. Owing to the decay of population of level 2, the up-conversion rate

$$C_{22,41}N_2^2\approx C_{22,41}N_1^2(W_{12}/R_2)^2$$

contains a factor R_2^{-2} which is not intrinsic to the up-conversion process. Hence, the intrinsic concentration dependence is given by $C_{22,41}N_1^2$. Since R_2 is relatively concentration independent, this is not an important distinction as far as the concentration dependence of the up-conversion rate is concerned. Taking I_{31} at 77°K from Fig. 8, R_2 from Fig. 9, and noting that $(R_{43}/R_4)(1+C_{41,22}N_1/R_4)^{-1}$ is relatively independent of concentration at 77°K yields

$$C_{22,41}N_1^2\propto I_{31}R_2^2\propto x^{2.8\pm0.2} \quad (12)$$

for $0.01<x<0.1$.

The result that the up-conversion rate has a concentration dependence essentially identical to the ion-pair decay rate agrees with the following theory. For the ion-pair process, Inokuti and Hirayama compute the time-dependent probability of finding an ion in the excited state after the ion has been excited.[25] With increasing time, the probability decreases both from spontaneous deactivation and the interaction with neighboring ground-state ions. Taking the appropriate statistical average over an ensemble of ions and integrating over time yields the average intensity. In the analogous theory for up-conversion the probability of an ion initially in the excited state decreases with time because of radiative decay and the interaction with other excited-state ions. Under steady-state pumping conditions, the excited-state population is a constant fraction of the total concentration. Hence, the concentration dependences of ion-pair decay and up-conversion will be identical if the interaction between the ions is the same in the two cases.

C. Effect of Migration

The above result is based on an essentially static excitation model. However, a third transfer process, that of migration of the excitation, may be present and can enhance the up-conversion efficiency. For example, the up-conversion process in anthracene involves the fusion of two triplet excitons to form a higher-energy singlet state, and the subsequent observation of singlet fluorescence.[26] The creation of singlets is governed primarily by the rate of collision of diffusing triplet excitons. The diffusion constant of the triplet exciton has been obtained from a measurement of the diffusion length and is 2×10^{-4} cm²/sec.

For a given ion-pair separation, resonant ion-pair decay and migratory transfer are expected to occur at about the same rates. However, if the excitation resides on an ion of a strongly coupled pair, and the pair is relatively well isolated from the other ions, ion-pair

relaxation will be rapid whereas the migration to other ions is much reduced. This can be a serious limit on the diffusion at low concentrations, but is expected to be less important at higher doping levels. Thus the rate for quenching is in general an upper limit on the migration rate.

If we assume the rate of migration is indeed given by the quenching rates in Fig. 10, the $^4I_{11/2}$ excitation undergoes numerous transfers before decay for $x>0.003$, and the excited $^4I_{11/2}$ population behaves as a dilute concentration of "particles" whose motion is described by a random walk. Under these conditions the up-conversion to $^4F_{7/2}$ is similar to the well-known coagulation of colloid particles in an electrolyte.[27] A static excitation samples a volume which is determined by the range dependence of the interaction and the lifetime of the state, whereas in the migration case the effective volume is the product of the mean free path and cross section. Since on the average an excited ion resides at a site a time $R_T^{-1} \ll R_2^{-1}$ the migration cross-section radius will generally be smaller than the radius of the interaction sphere for the static model. This further tends to reduce the effectiveness of migration in enhancing the up-conversion rate.

The diffusion constant of an excitation is

$$D = \langle r^2 \rangle_{\mathrm{av}} R_T/6, \tag{13}$$

where $\langle r^2 \rangle_{\mathrm{av}}^{1/2}$, the root mean-square displacement of a single transfer, is approximately equal to the average nearest-neighbor separation. For a 10% Er crystal, $\langle r^2 \rangle_{\mathrm{nn}}^{1/2} = 4.85$ Å and from Fig. 10, $R_T \sim 5\times10^6$ sec^{-1}, yielding $D \sim 2\times10^{-9}$ cm^2/sec. This is five orders of magnitude smaller than the triplet diffusion constant in anthracene, the difference being due to the vastly shorter scattering time of the triplets.[28] This explains why diffusion will be correspondingly less effective for Er^{3+} up-conversion.

Assuming diffusion dominates the up-transfer process, the transition from 2 to 4 is given by

$$C_{22,41} N_2^2 = 8\pi D L N_2^2, \tag{14}$$

where the additional factor 2 on the right-hand side accounts for the migration of both of the interacting particles. This assumes a hard-sphere model where each excitation is surrounded by a sphere of radius L to which a second ion must approach in order that they coalesce to form a $^4F_{7/2}$ state. For range-dependent interactions, L is a function of concentration. For example, for the dipole-dipole case it can be shown that $L \propto D^{-1/4}$.[29] If we assume the transfer rate is equal to the ion-pair rate, and thus proportional to $x^{2.9}$, we obtain, with $\langle r^2 \rangle_{\mathrm{av}} \propto x^{-2/3}$, that $D \propto x^{2.24}$ and from the above relationship $L \propto x^{-0.56}$. This is to be compared with the value of L obtained by solving Eq. (14):

$$L = C_{22,41} N_2^2 / 8\pi D N_2^2. \tag{15}$$

Substituting from Eq. (12) in the numerator and using the above concentration dependence of D in the denominator yields $L \propto x^{-1.43}$. The observation that the concentration dependence of L is stronger than for the dipolar case is consistent with the dependence of the transfer rate also being a more rapid function of concentration than dipolar. However, although migration can contribute, the results obtained from the concentration dependence do not allow us to extract the quantitative contribution of the effect of diffusion to the up-conversion efficiency.

D. Back Transfer at Higher Temperatures

At higher temperatures the ion-pair relaxation from $^2H_{11/2}$ is important and the concentration dependence is reduced. The decay partially repopulates $^4I_{11/2}$ via $^4I_{9/2}$, and we shall associate this decay with level 4 in our model. Neglecting differences in degeneracy, the steady-state population ratios N_2/N_1 and N_4/N_2 will be equal to W_{12}/R_2 and the intensity from level 3 will be linearly proportional to the concentration.[30] At 295°K the observed $^4S_{3/2}$ emission varies as $x^{1.3}$ for $0.01<x<0.1$ indicating the relaxation is intermediate between the fast and slow regimes described above.

IV. CONCLUSIONS

The spectroscopy of Er^{3+} in YF_3 and the temperature dependence of the emission have shown the conversion of 0.97μ radiation to 0.54-μ emission to be predominantly a resonant process involving the interaction between Er^{3+} ions in the $^4I_{11/2}$ state. Up-conversion involving transfer dominates the mechanism of consecutive absorption of two photons by a single ion for concentrations greater than 0.3%. The magnitude of the latter process is determined by the absorption strength of the $^4I_{11/2} \rightarrow {}^4F_{7/2}$ transitions. The situation for the transfer process is more complex. It is enhanced by the fact that an ion in the $^4I_{11/2}$ state can interact with a large number of neighboring ions, each of which has an equal probability to be excited to $^4I_{11/2}$ and to transfer its energy to an already excited ion. The relative strengths of the $^4I_{15/2} \rightarrow {}^4I_{11/2}$ and $^4I_{11/2} \rightarrow {}^4F_{7/2}$ absorptions are not known, but are presumably about equal. Hence, the degree of enhancement of the transfer process is proportional to the probability of finding a second excited ion among the ions with which the first excited ion can interact and the probability of transfer between these excited ions. The migration of the $^4I_{11/2}$ excitation can further enhance the number of effective neighbors.

This investigation has shown that up-conversion is essentially the inverse of ion-pair decay. The back transfer from $^4F_{7/2}$ can seriously degrade the over-all up-conversion efficiency since it competes with nonradiative $^4F_{7/2} \rightarrow {}^4S_{3/2}$ decay. However, at 295°K the most important reduction in the conversion efficiency

occurs from the thermal excitation from $^4S_{3/2} \rightarrow {}^2H_{11/2}$ and the ion-pair decay to $^4I_{9/2}$ and $^4I_{13/2}$.

These results also aid the understanding of the increased conversion efficiency obtained from the doubly doped YF_3:Yb^{3+}, Er^{3+} phosphors. The radiative efficiencies of the Yb^{3+} $^4F_{5/2} \rightarrow {}^4F_{7/2}$ and Er^{3+} $^4I_{11/2} \rightarrow {}^4I_{15/2}$ transitions are high. The relative lifetimes of the two transitions indicates the Yb^{3+} absorption is about a factor 5 stronger than the Er^{2+} absorption. Of equal importance is the observation that Yb^{3+} is appreciably less effective than Er^{3+} itself in the quenching of $^4S_{3/2}$ emission by ion-pair decay.[31] The smaller ion-pair decay of the (Er, Yb) system results from the

$$(^4S_{3/2}, {}^2F_{7/2}) \rightarrow (^4I_{13/2}, {}^2F_{5/2})$$

transition which involves the emission of $\sim$2000 cm^{-1} of energy. The first of the two effects compensates for the reduction of the infrared lifetime, while the second produces a major fraction of the enhancement in the up-conversion efficiency.

In addition, the Yb^{3+} and the Er^{3+} doping levels can be independently varied to obtain the optimum efficiency. Making use of the similarity of the properties of Yb^{3+} and Er^{3+} infrared levels, we can obtain the best doping level from the Er^{3+} data. From Fig. 7 the maximum $^4S_{3/2}$ emission occurs at $\sim$1% concentration for $^4F_{7/2}$ excitation and, from Fig. 8, at $\sim$20% for $^4I_{11/2}$ excitation. These are the observed optimum concentrations for Er^{3+} and Yb^{3+}, respectively, of the doubly doped system.[31]

ACKNOWLEDGMENTS

We are grateful to J. E. Geusic and R. C. Miller for helpful discussions and to F. L. Clark and W. H. Grodkiewicz for technical assistance.

[1] V. V. Ovsyankin and P. P. Feofilov, Zh. Eksperim. i Teor. Fiz. Pis'ma v Redaktsiyu **3,** 494 (1966) [Soviet Phys. JETP Letters **3,** 322 (1966)]; P. P. Feofilov and V. V. Ovsyankin, Appl. Opt. **6,** 1828 (1967).

[2] R. J. Woodward, J. M. Williams, and M. R. Brown, Phys. Letters **22,** 435 (1966).

[3] M. R. Brown, W. A. Shand, H. Thomas, and J. S. S. Whiting, J. Chem. Phys. **50,** 881 (1969); M. R. Brown, H. Thomas, J. M. Williams, and R. Woodward, *ibid.* **51,** 3321 (1969).

[4] E. Chicklis and L. Esterowitz, Phys. Rev. Letters **21,** 1149 (1968).

[5] F. Auzel, Compt. Rend. **262B,** 1016 (1966); **263B,** 819 (1966).

[6] R. A. Hewes and J. F. Sarver, Phys. Rev. **182,** 427 (1969).

[7] R. A. Hewes, in *Proceedings of the International Conference on Luminescence, Newark, Del., 1969,* edited by F. Williams (North-Holland, Amsterdam, 1970), p. 778; J. Luminescence **11,** 778 (1970).

[8] V. V. Ovsyankin and P. P. Feofilov, Zh. Eksperim. i Teor. Fiz. Pis'ma v Radaktsiyu **4,** 471 (1966) [Soviet Phys. JETP Letters **3,** 317 (1966)].

[9] L. G. Van Uitert, S. Singh, H. J. Levinstein, L. F. Johnson, W. H. Grodkiewicz, and J. E. Geusic, Appl. Phys. Letters **15,** 53 (1969).

[10] L. F. Johnson, J. E. Geusic, H. J. Guggenheim, T. Kushida, S. Singh, and L. G. Van Uitert, Appl. Phys. Letters **15,** 48 (1969).

[11] H. J. Guggenheim and L. F. Johnson, Appl. Phys. Letters **15,** 51 (1969).

[12] L. G. Van Uitert, L. W. Pictrosky, and W. H. Grodkiewicz, Mater. Res. Bull. **4,** 777 (1969).

[13] A. Zalkin and D. H. Templeton, J. Am. Chem. Soc. **75,** 2453 (1953).

[14] Recent measurements on (YYbEr)F_3 show the green emission to have a quadratic dependence on absorption when $A<0.5$ in agreement with the present results: J. E. Geusic (private communication).

[15] L. G. Van Uitert, E. F. Dearborn, and J. J. Rubin, J. Chem. Phys. **47,** 3653 (1967).

[16] M. J. Weber, Phys. Rev. **156,** 231 (1966); **157,** 262 (1967).

[17] The theory of energy transfer has been developed by D. L. Dexter, J. Chem. Phys. **21,** 836 (1954); and D. L. Dexter and J. H. Schulman, *ibid.* **22,** 1063 (1954).

[18] R. Orbach, in *Optical Properties of Ions in Crystals,* edited by H. M. Crosswhite and H. W. Moos (Wiley, New York, 1967), p. 445.

[19] L. G. Van Uitert, J. Electrochem. Soc. **114,** 1048 (1967).

[20] R. J. Birgeneau, J. Chem. Phys. **50,** 4282 (1969).

[21] W. B. Gandrud and H. W. Moos, J. Chem. Phys. **49,** 2170 (1968).

[22] I. A. Nagibarova and V. R. Nagibarov, Zh. Eksperim. i Teor. Fiz. **55,** 1277 (1969) [Soviet Phys. JETP **28,** 669 (1969)].

[23] V. M. Agranovich, Opt. i Spektroskopiya **9,** 113 (1960) [Opt. Spectry. (USSR) **9,** 59 (1960)]; *ibid.* **9,** 798 (1960) [*ibid.* **9,** 421 (1960)].

[24] J. D. Dow, Phys. Rev. **174,** 962 (1968).

[25] M. Inokuti and F. Hirayama, J. Chem. Phys. **43,** 1978 (1965).

[26] V. Ern, P. Avakian, and R. E. Merrifield, Phys. Rev. **148,** 872 (1966).

[27] S. Chrandraskhar, Rev. Mod. Phys. **15,** 1 (1943).

[28] P. Avakian, V. Ern, R. E. Merrifield, and A. Suna, Phys. Rev. **165,** 974 (1968).

[29] M. Yokota and O. Tanimoto, J. Phys. Soc. Japan **22,** 779 (1967).

[30] The analogous problem in the Yb-Er-doped fluorides was considered by J. D. Kingsley, G. E. Fenner, and S. V. Galginaitis, Appl. Phys. Letters **15,** 115 (1969); J. D. Kingsley, J. Appl. Phys. **41,** 175 (1970).

[31] J. P. van der Ziel, F. W. Ostermayer, Jr., and L. G. Van Uitert (unpublished).